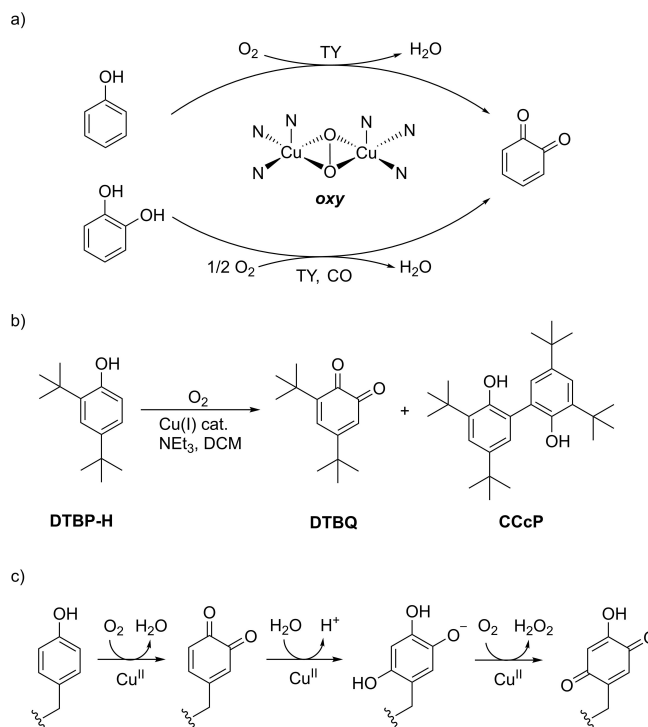**Copper Catalysis** | **Hot Paper**

Copper-Catalyzed Monooxygenation of Phenols: Evidence for a Mononuclear Reaction Mechanism

Rebecca Schneider, Tobias A. Engesser,* Christian Näther, Ingo Krossing, and Felix Tuczek*

Abstract: The Cu^I salts [Cu(CH$_3$CN)$_4$]**PF** and [Cu-(oDFB)$_2$]**PF** with the very weakly coordinating anion Al(OC(CF$_3$)$_3$)$_4^-$ (**PF**) as well as [Cu(NEt$_3$)$_2$]**PF** comprising the unique, linear bis-triethylamine complex [Cu-(NEt$_3$)$_2$]$^+$ were synthesized and examined as catalysts for the conversion of monophenols to *o*-quinones. The activities of these Cu^I salts towards monooxygenation of 2,4-di-*tert*-butylphenol (DTBP-H) were compared to those of [Cu(CH$_3$CN)$_4$]X salts with "classic" anions (BF$_4^-$, OTf$^-$, PF$_6^-$), revealing an *anion effect* on the activity of the catalyst and a *ligand effect* on the reaction rate. The reaction is drastically accelerated by employing Cu^{II}-semiquinone complexes as catalysts, indicating that formation of a Cu^{II} complex precedes the actual catalytic cycle. This result and other experimental observations show that with these systems the oxygenation of monophenols does not follow a dinuclear, but a mononuclear pathway analogous to that of topaquinone cofactor biosynthesis in amine oxidase.

Introduction

Copper-containing enzymes catalyze a variety of biological oxidation and oxygenation reactions.[1–3] One important enzyme in this context is tyrosinase (TY, Scheme 1a). This type3 copper enzyme mediates the hydroxylation and subsequent two-electron oxidation of L-tyrosine to L-dopaquinone, corresponding to the first step of melanin biosynthesis.[1,4–6] The related enzyme catechol oxidase,

[*] R. Schneider, Dr. T. A. Engesser, Prof. Dr. C. Näther,
    Prof. Dr. F. Tuczek
    Institut für Anorganische Chemie,
    Christian-Albrechts-Universität zu Kiel
    Max-Eyth-Straße 2, 24118 Kiel (Germany)
    E-mail: tengesser@ac.uni-kiel.de
        ftuczek@ac.uni-kiel.de

    Prof. Dr. I. Krossing
    Institut für Anorganische und Analytische Chemie,
    Albert-Ludwigs-Universität Freiburg
    Albertstraße 21, 79104 Freiburg (Germany)

Scheme 1. a) Reactions performed by tyrosinase (TY) and catechol oxidase (CO). Centre: schematic drawing of the *oxy*-form of the active site. b) Catalytic reaction of the phenolic substrate DTBP-H to *o*-quinone DTBQ and CC-coupling side product CCcP. c) Topaquinone cofactor biosynthesis mediated by the mononuclear Cu^{II} centre of amine oxidase (AO).

lacking monophenolase activity, generates L-dopaquinone by oxidation of L-dopa.[6,7] Melanin plays an important role in UV-protection, immune response and wound healing in plants and animals.[8] Key information regarding the reactivity of TY has been obtained from small-molecule model systems, and small structural changes have often been found to have a major impact on their activity.[1] The first catalytic system was developed by Réglier et al., being able to convert 2,4-di-*tert*-butylphenol (DTBP-H) to 3,5-di-*tert*-butylquinone (DTBQ) (Scheme 1b).[9] Over the years further catalytic TY model systems, all with at least bidentate *N*-donor ligands, were developed and investigated regarding their properties by Casella et al.,[10] Stack et al.,[11,12] Ottenwaelder and Lumb et al.,[13,14] Herres-Pawlis et al.[15–17] and others.[7,18]

The fundamental mechanism of TY activity, proceeding via a *μ-η²:η²*-peroxo-dicopper(II) species, has been firmly rooted in the literature for decades (Scheme 1a). The

formation and detection of corresponding intermediates as well as their impact on catalytic activity thus have always been of central importance in TY model chemistry.[6,12,15,17,19,20] In order to obtain more information about the factors influencing the performance of the catalysts, our group focused on the improvement of TY model compounds based on mononuclear copper(I) complexes. Within this project steric and electronic effects of primarily applied bidentate *N*-donor ligands were investigated in detail.[5,6,20–24] Catalytic runs usually involve 50 equiv of monophenol along with 100 equiv of NEt$_3$ with respect to a mononuclear Cu^I precursor (*Bulkowski-Réglier conditions*).[9,25] Nevertheless, conversion of the starting monophenol to the desired *o*-quinone was always found to be far from complete.[5,6,20,23,24] In order to explain the low turnover numbers, we looked for possible decomposition pathways of the catalysts leading to dead-end species. In this context, the dinuclear Cu^{II} complex [Cu$_2$(μ-F)(**dmPMP**)$_4$]-(PF$_6$)$_3$ (**dmPMP** = 2-[(3,5-dimethyl-1*H*-pyrazol-1-yl)methyl]pyridine) was isolated from the pyrazole-based **dmPMP** system that exhibited a comparatively low (11%) conversion of DTBP-H to DTBQ.[23] Importantly, the bridging fluoride anion can only originate from the PF$_6^-$ counterion, indicating that an instability of the anion may indeed lower the catalytic activity of such a TY model system.[23]

Herein, we first report on the influence of counterions on the catalytic activity of copper(I) complexes regarding the monooxygenation of phenols (*anion effect*). To this end we examine a series of simple copper(I) salts containing the same ligands, but different anions as catalysts for this reaction. We demonstrated earlier that, besides the well-described activity of systems containing bi- and tridentate ligands, simple [Cu(CH$_3$CN)$_4$]PF$_6$ also exhibits tyrosinase-like activity.[23] So we use different [Cu(CH$_3$CN)$_4$]X salts (**1-X**; X = BF$_4^-$, OTf$^-$, PF$_6^-$ and Al(OC(CF$_3$)$_3$)$_4^-$ = **PF**, cf Scheme 2) for the catalytic monooxy-genation of phenols, focusing on the conversion of DTBPH to DTBQ (Scheme 1b).
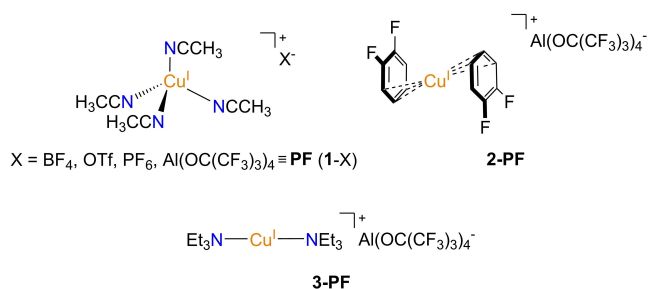
Whereas the BF$_4^-$, OTf$^-$ and PF$_6^-$ salts comprise "classic" medium- to weaker-coordinating anions, **PF** represents a very weakly coordinating anion that both proved to be stable towards dissociation[26,27] and in multiple cases led to increased catalytic activities.[28,29] Notably, such a very weakly coordinating anion has never been used before in reactivity studies of copper monooxygenase models. Having

examined the influence of the anion, we will then vary the ligand environment of the Cu^I complexes and in this context compare **1-PF** with [Cu(*o*DFB)$_2$]**PF** (**2-PF**, *o*DFB = 1,2-difluorobenzene) and [Cu(NEt$_3$)$_2$]**PF** (**3-PF**) regarding their catalytic monooxygenase activities (*ligand effect*). Notably, **3-PF** contains the first linear Cu^I complex coordinated by two tertiary monoamine ligands and also represents the first homoleptic metal complex with these ligands (Scheme 2). Based on detailed experimental evidence, a mechanism for the monooxygenation of phenols catalyzed by **1-**, **2-** and **3-PF** is proposed. In contrast to the well-established, dinuclear mechanism of TY (Scheme 1a), the hypothetical pathway is mononuclear and corresponds to the (stoichiometric) topaquinone (TPQ) cofactor biosynthesis in the enzyme amine oxidase (AO, cf Scheme 1c).[30–33] The post-translational conversion of a nearby tyrosine to the TPQ cofactor of its mononuclear copper active site is an additional feature to the primary function of this enzyme, the oxidation of amines to aldehydes.[3,30,32–35] Importantly, the biosynthesis of TPQ represents the second known pathway (besides TY) for a copper-mediated monooxygenation of phenols in nature and to date has not been observed in a catalytic fashion, neither in biology nor in synthetic chemistry. Therefore, the results presented herein establish a new, mononuclear scenario for the catalytic conversion of monophenols to *o*-quinones in biomimetic copper chemistry.

Results and Discussion

To study the influence of the counterion (*anion effect*) on the catalytic activity of simple copper salts regarding the monooxygenation of phenols, we first employed the series of Cu^I acetonitrile complexes [Cu(CH$_3$CN)$_4$]X (**1-X**) containing anions X of variable coordination strength and stability (X = BF$_4^-$, OTf$^-$, PF$_6^-$). Importantly, the salts with BF$_4^-$ and OTf$^-$, both slightly stronger coordinating than PF$_6^-$,[36] showed 7% and, resp., 11% yield, lower than the PF$_6^-$ system which gave 15% yield (Table 1 and Figure 1a). A similar trend was observed for the reaction rate which was also found to increase in the sequence BF$_4^-$ < OTf$^-$ < PF$_6^-$, concomitant with a decreasing anion coordinating ability.[27] This suggests that the anion affects the catalytic activity through coordination to the metal center, which causes blocking of the active site and lowers the reaction rate. A second factor decreasing the yield may be a decomposition of the anion, leading to destruction of the catalyst and formation of dead-end species like the μ-fluorido complex [Cu$_2$(μ-F)(**dmPMP**)$_4$](PF$_6$)$_3$ (see above).[23]

In order to eliminate the described *anion effect* as far as possible, the inert, unreactive and very weakly coordinating anion Al(OC(CF$_3$)$_3$)$_4^-$ (**PF**) was employed.[37,38] The corresponding copper(I) salt [Cu(CH$_3$CN)$_4$]**PF** (**1-PF**) has been synthesized in the past by metathesis with the corresponding Li$^+$, Tl$^+$ and Ag$^+$ salts.[29,39] These syntheses generate at least one other metal salt (e.g. AgCl)[29,39] as by-product, introducing a potential impurity which in turn may affect the catalytic activity. On the other hand, reaction of elemental copper with the metal-free oxidant [NO]**PF** was found to

X = BF$_4$, OTf, PF$_6$, Al(OC(CF$_3$)$_3$)$_4$ ≡ **PF** (**1-X**)　　**2-PF**

3-PF

Scheme 2. Copper(I) salts employed for the conversion of DTBP-H to DTBQ in this study.

Table 1: Tyrosinase-like activity for the conversion[a] of DTBP-H, mediated by [CuL$_n$]X salts (L=CH$_3$CN, n=4, X=BF$_4$, OTf, PF$_6$, **PF** (**1**-X); L=*o*DFB, NEt$_3$, n=2, X=**PF** (**2-PF** and **3-PF**)) and with a copper(II)-semiquinone complex directly generated in situ starting from **1-PF** or **2-PF** and DTBQ.

	[Cu(CH$_3$CN)$_4$]$^+$				[Cu(*o*DFB)$_2$]$^+$	[Cu(NEt$_3$)$_2$]$^+$		
	BF$_4^-$	OTf$^-$	PF$_6^-$	Al(OC(CF$_3$)$_3$)$_4^-$ (**1-PF**)	Al(OC(CF$_3$)$_3$)$_4^-$ (**2-PF**)	Al(OC(CF$_3$)$_3$)$_4^-$ (**3-PF**)	**1-PF**+DTBQ (**1^{SQ}-PF**)	**2-PF**+DTBQ (**2^{SQ}-PF**)
yield/% (5h)[b]	7	11	15	38	39	40	40	40
reaction rate/10^{-4} M min^{-1}								
0–5 min	0.65±0.08	1.28±0.11	1.48±0.11	1.57±0.12	0.47±0.07	0.45±0.07	3.52±0.20	2.96±0.18
0–15 min	0.34±0.02	0.62±0.03	1.26±0.04	1.95±0.05	1.14±0.04	0.95±0.03	2.92±0.07	3.19±0.07
0–30 min	0.24±0.01	0.44±0.01	0.86±0.02	1.79±0.03	1.48±0.02	1.31±0.02	2.21±0.03	2.29±0.03
ratio of products[c]	88:6:6	66:9:25	81:14:5	49:40:11	50:39:11	48:42:10	43:45[d]:11	46:41[d]:12

[a] The reactions were carried out under *Bulkowski-Regliér conditions*,[9,25] using a solution of the Cu^I salt (500 μM), DTBP-H (25 mM) and NEt$_3$ (50 mM) in DCM. [b] The yield in relation to the substrate quantity was determined via UV/Vis spectroscopy. [c] The ratio of the reaction products DTBP-H:DTBQ:CCcP (CCcP=3,3′,5,5′-tetra-*tert*-butyl-2,2′-biphenol) was calculated from the ^{1}H-NMR spectra. [d] The determined amount of DTBQ was reduced by 1, since an equivalent was already present at the beginning of the reaction.

Figure 1. UV/Vis spectra measured during the oxygenation of a solution of a) [Cu(CH$_3$CN)$_4$]OTf, b) [Cu(CH$_3$CN)$_4$]**PF** (**1-PF**), c) [Cu(NEt$_3$)$_2$]**PF** (**3-PF**) in DCM (500 μM each) in the presence of DTBP-H (25 mM) and NEt$_3$ (50 mM) during the first 5 h at room temperature; quartz cell length *l*=0.1 cm. Bottom: Corresponding yield in relation to the substrate quantity (black dots) and reaction rate (red triangles) as function of time.

provide access to the target compound in high purity and free of other metal salts (Scheme 3), analogous to the results of Hayton and Underhill et al.[40] The obtained [Cu-(CH$_3$CN)$_4$]**PF** (**1-PF**) proved to be highly active regarding the monooxygenation of DTBP-H, as evidenced by a strongly increased yield of 38%, which represents the highest value observed with this substrate so far (Figure 1b). Notably, in all of these reactions the C–C coupling product CCcP is formed to some extent (cf Scheme 1 and Table 1). Its relative yield, however, is much lower for the salts with **PF** (22%) as compared to those with classic anions (50% (BF$_4^-$), 74% (OTf$^-$), 26% (PF$_6^-$)), indicating that **1-PF** is also more *selective* than the other systems. Finally, **PF** further accelerates the reaction, leading to a reaction rate increasing in the sequence X=BF$_4^-$<OTf$^-$<PF$_6^-$<**PF** (Table 1). This indicates that the anion affects both the product yield and the reaction rate, probably by competing with the substrate for the binding site at the metal center (*anion effect*).

Scheme 3. Synthesis of the copper salts used in this study.

As **PF** already represents one of the most stable and least coordinating anions, it is likely that the reaction rate cannot be increased much further by changing the anion. Therefore, the question arose as to what extent the *ligand* influences the reactivity and whether a weaker coordinating ligand than acetonitrile may lead to a higher activity. Notably, such a system would combine the effect of a stable and very weakly coordinating anion with a highly reactive copper(I) center, leading both to high yields and reaction rates. In 2009, one of us presented such a system with [Cu(*o*DFB)$_2$]**PF** (**2-PF**), combining the weakly binding ligand 1,2-difluorobenzene (*o*DFB) with a weakly coordinating counterion.[37] However, like in the case of **1-PF**, a salt metathesis with CuI, AgF and Li**PF** in *o*DFB was employed for the synthesis of **2-PF**, leading to silver impurities. Therefore, we applied our new protocol of oxidizing elemental copper with [NO]**PF** to the synthesis of the latter complex, but this time in *o*DFB (Scheme 3). This successfully led to highly pure [Cu(*o*DFB)$_2$]**PF** (**2-PF**) and allowed measurement of a Raman spectrum of this compound for the first time (Figure S1).

Conversion of DTBP-H to DTBQ catalyzed by **2-PF** under *Bulkowski-Réglier conditions*[9,25] gave a yield of 39 %, almost the same value as obtained for **1-PF**. However, the reaction rate for the first 5 minutes was significantly lower than observed for the latter, even below the value of **1**-BF$_4$. These results indicate a *ligand effect* influencing the reaction rate, as opposed to the *anion effect*, which leads to increased yields and reaction rates with weaker coordination ability of the anion when the same ligand is used. To shed light on the origin of this *ligand effect*, the catalytic process has to be considered in more detail. Especially in case of **2-PF**, it is highly probable that during catalysis the weakly bound *o*DFB is exchanged by NEt$_3$ of which 100 equiv are also added under the chosen conditions (see above),[9,25] primarily to deprotonate the employed monophenol;[5] but it may also act as a ligand.

To examine whether a NEt$_3$ complex is initially formed when **2-PF** is employed as catalyst, we tried to directly synthesize a [Cu(NEt$_3$)$_x$]$^+$ salt. Again, **PF** was chosen as counterion. As no homoleptic monoamine complex with any metal ([M(NR$_3$)$_x$]$^{n+}$, R = alkyl) has been structurally characterized so far, it was unclear whether a direct synthesis of [Cu(NEt$_3$)$_x$]**PF** is feasible. There are a few examples of compounds containing chelating diamine ligands[41] or the linear ammine complex [Cu(NH$_3$)$_2$]$^+$,[42] which indicated that an analog with acyclic monoamine ligands could be accessible. A first attempt to synthesize the target compound in analogy to **1-** and **2-PF** by oxidation of copper did not lead to a well-defined product, probably due to decomposition of the anion and/or oxidation of the amine (Scheme 3, for more detail see Supporting Information).

Therefore, this complex was prepared by ligand exchange of **2-PF** with NEt$_3$ in DCM (Scheme 3). This led to [Cu(NEt$_3$)$_2$]**PF** (**3-PF**) in phase-pure form according to XRPD (Figure S7). Moreover, this new compound could be structurally (Figure 2) and spectroscopically (Figure S3–S6) characterized (for more details see Supporting Information). The crystal structure shows an almost perfectly linear
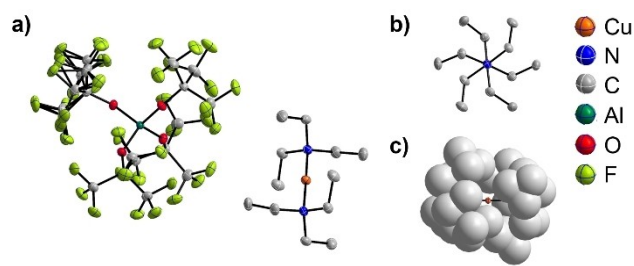

Figure 2. a) Molecular structure of [Cu(NEt$_3$)$_2$]**PF** (**3-PF**), b) view on the N–Cu–N axis of the [Cu(NEt$_3$)$_2$]$^+$ cation (H atoms are omitted for clarity) and c) the interdigitated ethyl groups shielding the copper center (H atoms with space filling model).

(N1–Cu1–N11 178.84(6)°) Cu^I complex with two amine ligands exhibiting tetrahedral geometry at the nitrogen atoms (Cu1–N1–C1/3/5 109.78(11)°/111.25(11)°/110.04-(11)°).[43]

The cation has overall S_6 molecular symmetry, almost identical to the calculated gas phase geometry, which can be attributed to the anion and its very weak secondary interaction to the cation (Figure S54).[44]

Thus, with **3-PF** we were able to obtain the first structurally characterized, homoleptic monoamine metal complex. Regarding the relative stabilities in the series of homoleptic [Cu(NEt$_3$)$_x$]$^+$ complexes with $x = 2$, 3 and 4, DFT calculations show that the bis-amine complex [Cu(NEt$_3$)$_2$]$^+$ is the only stable one, as optimization of the tris- and tetrakis-complexes leads to decoordination of one or, resp., two amine ligands. With a difference of -186 kJ mol^{-1} in the gas phase and -157 kJ mol^{-1} in DCM solution (Figure S52, S53), [Cu(NEt$_3$)$_2$]$^+$ should also be much more stable than [Cu(*o*DFB)$_2$]$^+$ and therefore should be directly accessible from the latter (for more details see Supporting Information), in agreement with the experimental findings (see below). Oxygenation of DTBP-H in the presence of **3-PF** leads to the formation of DTBQ in 40 % yield, which again is practically the same value as in the presence of **1-** or **2-PF** (Table 1, Figure 1c). This confirms that influences of anion coordination and dissociation on the attainable yields are absent in these three systems, in contrast to their analogs with "classic" anions (BF$_4^-$, OTf$^-$ and PF$_6^-$, cf Figure 3). However, the ligands influence the *initial rates* of the catalytic reaction (cf Table 1).

Further information on these issues is provided by monitoring the time dependence of the reaction rate for all catalytic reactions over a longer period (180 min., Figure 4). As evident from this Figure, the rate goes through a maximum for **1-**, **2-** or **3-PF**, reflecting the presence of an induction period before the maximum activity is reached. The actual catalytically active species thus forms from the Cu^I salts **1-**, **2-** or **3-PF** but at different rates depending on their ligands (CH$_3$CN (**1-PF**), *o*DFB (**2-PF**) or NEt$_3$ (**3-PF**)), which means that these complexes are in fact precatalysts. Notably, the absolute values of the rates and their time course are almost identical for **2-** and **3-PF**, suggesting that a rapid ligand exchange in **2-PF**, in situ generating **3-PF**, occurs in the presence of NEt$_3$ (Figure 4). This hypothesis is
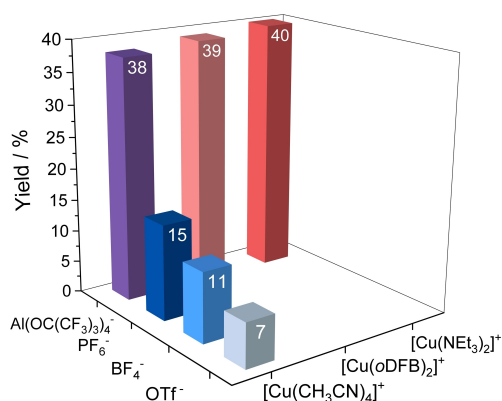
Angew. Chem. Int. Ed. **2022**, *61*, e202202562 (4 of 9)

© 2022 The Authors. Angewandte Chemie International Edition published by Wiley-VCH GmbH

Figure 3. Yields of DTBQ achieved upon reaction of DTBP-H (25 mM) with O₂ in the presence of NEt₃ (50 mM) and different Cuᴵ salts (500 μM) after 5 h as function of the counterion and the complex cation.
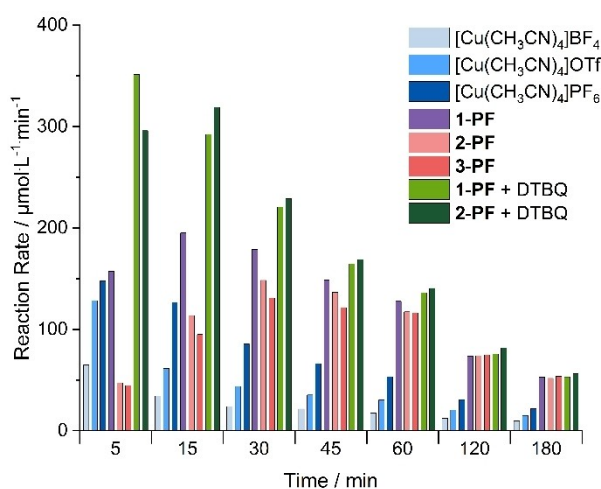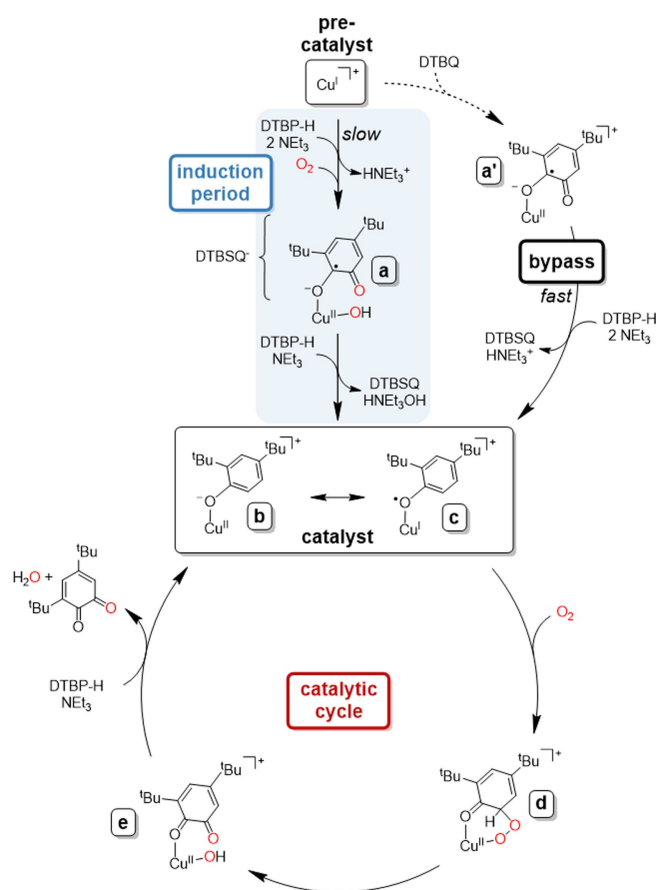

Figure 4. Reaction rates of the oxygenation of DTBP-H (25 mM) to DTBQ catalyzed by different Cuᴵ salts (500 μM) in the presence of NEt₃ (50 mM) during the first 3 h.

In order to rationalize the experimental findings, a mechanistic cycle is proposed (Scheme 4). Accounting for the observed induction period, it starts at the level of Cuᴵ salts which oxygenate the first substrate molecule in a preliminary reaction sequence (Scheme 4, top), forming the active catalyst of the actual catalytic reaction (Scheme 4, bottom). Whereas the preliminary reaction sequence may proceed through a mono- or a dinuclear mechanism (see below), the actual catalytic cycle cannot be dinuclear as it is based on Cuᴵᴵ, precluding formation of a μ-η^2:η^2-peroxo intermediate from two Cuᴵ centers and O₂. Instead, it can be anticipated to follow the other known scenario of phenol monooxygenation in nature, the biosynthesis of TPQ in AO, which is mononuclear (see above).[30–35, 45, 46] According to these considerations, we assume that during the induction period, the Cuᴵ salt reacts with O₂ and one substrate molecule to form a Cuᴵᴵ-semiquinone complex (Scheme 4a). Addition of substrate and base to this species leads to liberation of 3,5-di-*tert*-butylsemiquinone (DTBSQ) and formation of a phenolate-copper(II) complex (Scheme 4b), starting the actual catalytic cycle. Following the mechanism of TPQ biosynthesis,[32, 35, 45] the phenolate ligand in intermediate **b** converts to a phenoxyl radical, reducing Cuᴵᴵ to Cuᴵ. The Cuᴵ phenoxyl complex (Scheme 4c) reacts with O₂ to give **d**, a bridging peroxo intermediate, which is

also in accordance with the calculated energies of these complexes (see above). By contrast, if **1-PF** is employed as (pre)catalyst, the reaction rate is significantly higher compared to **2**- and **3-PF** at the beginning of the reaction, and the maximum is reached at shorter reaction times. Afterwards, it decreases again, approaching similar rates as **2**- and **3-PF**. This suggests that the reactive species is formed faster with **1**- than with **2**- or **3-PF**, which is compatible with the fact that the initial reaction rates are higher for *all* **1-X** salts (with **X** = BF₄⁻, OTf⁻, PF₆⁻ and **PF**) than for **2**- and **3-PF** (Figure 4). However, the reaction rate of **1-PF** exceeds the rates of the other **1-X** salts, and it goes through a maximum in the course of the reaction, whereas for the other **1-X** systems the rates monotonically decrease from the beginning. This indicates that the "full" catalytic activity of the [Cu(CH₃CN)₄]⁺ complex requires the presence of the aluminate counterion, whereby an induction period applies to reach that activity.

Scheme 4. Proposed mechanism for the conversion of DTBP-H to DTBQ, starting from simple Cuᴵ salts. For clarity, the counterion and additional ligands such as CH₃CN or NEt₃ have been omitted.

Angew. Chem. Int. Ed. **2022**, *61*, e202202562 (5 of 9)

© 2022 The Authors. Angewandte Chemie International Edition published by Wiley-VCH GmbH

subsequently transformed to the *o*-quinone complex (Scheme 4e) by O–O cleavage. Addition of base and substrate releases the product and closes the catalytic cycle. In order to investigate the starting point or identify an early intermediate of the proposed mechanism (Scheme 4), a stoichiometric reaction of sodium 2,4-di-*tert*-butylphenolate (NaDTBP) and O_2 in presence of **3-PF** was performed, avoiding actually entering the turnover regime. The use of **3-PF** ensures that the necessary NEt_3 is present as coligand during the reaction, like under catalytic *Bulkowski-Réglier conditions*,[9;25] but without excess, which could lead to replacement of the bound substrate.

The UV/Vis spectra of this reaction initially show a shoulder between 350 and 500 nm slowly increasing in intensity (Figure 5 **top**). As the reaction proceeds, a double band feature with maxima at 385 and 400 nm and a broad shoulder at ≈ 430 nm emerges which previously has been attributed to free DTBSQ.[22] In agreement with this, an EPR spectroscopic analysis of the reaction solution shows
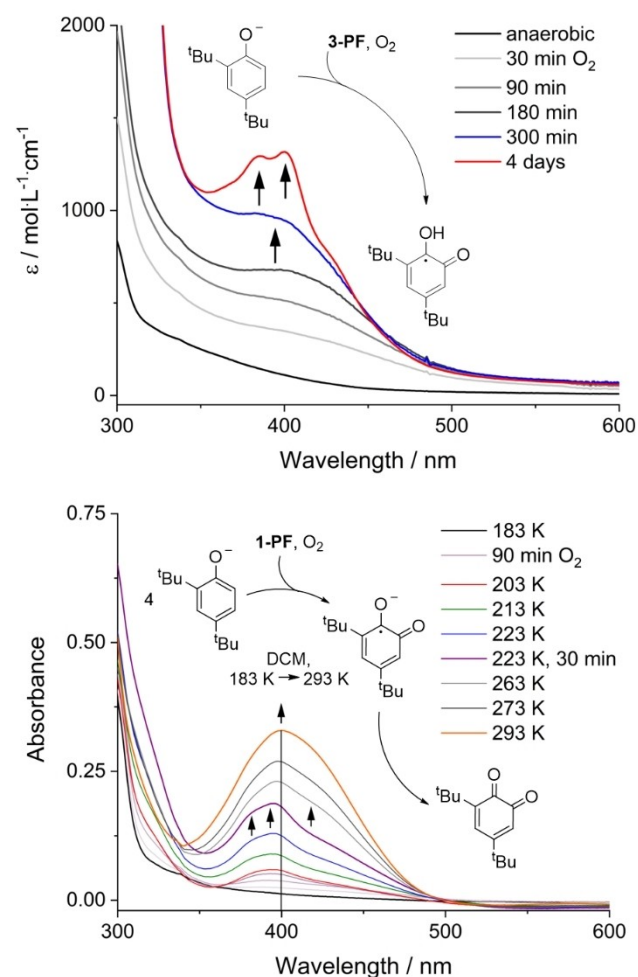
the presence of an organic radical (Figure S40). The formation of semiquinone (SQ) was further confirmed by a stoichiometric reaction of DTBP-H and NEt_3 with **2-PF** and O_2 (Figure S41).

To check whether SQ is also formed under (quasi-) catalytic conditions, the oxygenation was performed with **1-PF** in the presence of a slight excess of DTBP-H (4 equiv) and NEt_3 (4 equiv) at low temperatures, in order to detect possible intermediates. The UV/Vis spectra measured under these conditions resemble the one of the stoichiometric reaction, exhibiting an absorption feature at 397 nm as well as two shoulders at ≈ 385 and ≈ 430 nm (Figure 5 bottom, Figure S42 for similar experiments with **2-PF**). Upon heating up to room temperature a bathochromic shift of the absorption occurs and the characteristic quinone band of the product DTBQ evolves at 405 nm. These findings indicate that the formation of SQ precedes the formation of quinone and implies the presence of a copper-based oxygenation reaction, which is in accordance with the proposed induction period (Scheme 4 top).

If a SQ-complex is part of the mechanistic scenario and is formed during the induction period, using a Cu^{II}-SQ complex (Scheme 4, **a′**) directly as catalyst should significantly increase the reaction rate by bypassing the slow conversion of the precatalyst to the catalyst (Scheme 4, dotted arrows). To check this hypothesis, a Cu^{II}-SQ complex (**1^SQ-PF**), directly generated in situ from **1-PF** and DTBQ (Scheme 4, **a′**), was employed as a catalyst for the oxygenation of DTBP-H. In fact, catalytic conversion to DTBQ occurred with the same yield as observed for the parent Cu^I complex **1-PF** (Table 1), but with a considerably higher initial reaction rate (Figure 4, green bars). Importantly, the high initial reaction rate does not increase further in the course of the reaction, passing through a maximum (as for **1-PF** itself), but *decreases* monotonically in the course of the reaction. This shows that the induction period of the catalytic reaction now is eliminated, which in turn confirms that it involves oxygenation of one phenol to SQ, being accompanied with the oxidation of Cu^I to Cu^{II} (Scheme 4 top). Analogous investigations with **2-PF** and **2^SQ-PF** lead to similar results (Figure S21–S23). In contrast to **1^SQ-PF**, a maximum of the reaction rate is observed for **2^SQ-PF** after 15 minutes. This lag is caused by the addition of NEt_3, leading to release of DTBQ and probably formation of thermodynamically favored **3-PF** (Figure S21–S23).

Electronic absorption data of free DTBSQ are scarce. Only one publication gives absorption maxima of neutral DTBSQ, but no extinction coefficients are quoted.[47] In order to further characterize DTBSQ, **2^SQ-PF** was protonated with $HNEt_3PF$ in the presence of 1 equiv NEt_3 as additional ligand. This led to disappearance of the absorption maxima observed for **2^SQ-PF** (377 nm/1727 mol L^{-1} cm^{-1}, 485 nm/2179 mol L^{-1} cm^{-1}), whereas at 297 nm (7369 mol L^{-1} cm^{-1}) and 396 nm (2398 mol L^{-1} cm^{-1}) two new absorption maxima appeared (Figure 6). The band shape of the feature at 396 nm resembles that of free DTBSQ obtained from oxygenation of DTBP-H in the presence of **3-PF** and **1-PF** (see above, Figure 5 top and bottom), implying that protonation of **2^SQ-PF** leads to release of DTBSQ. After
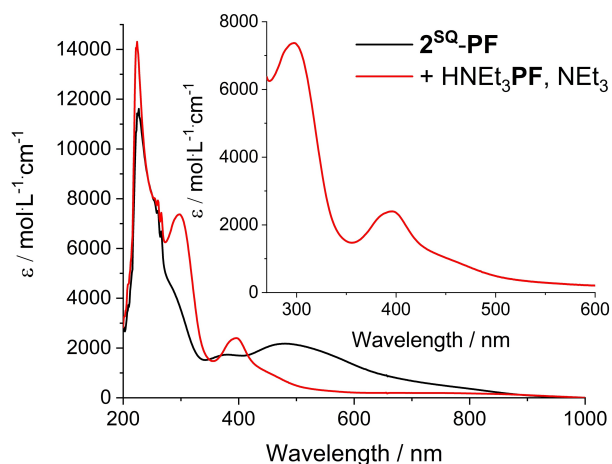
Figure 5. Top: UV/Vis spectra measured upon conversion of NaDTBP (500 μM) in DCM in the presence of **3-PF** (500 μM) during 4 days. Bottom: UV/Vis spectra measured during the oxygenation of **1-PF** (500 μM, DCM) in the presence of 4 equiv DTBP-H and 4 equiv NEt_3 at a temperature range from 183–293 K.

Figure 6. UV/Vis spectra of the reaction of **2^{SQ}-PF** (1.5 mM) with one equivalent each of HNEt₃**PF** and NEt₃ (1.5 mM) in DCM; Inset: enlarged view of the UV/Vis-spectrum of **2^{SQ}-PF** after protonation.

Figure 7. Dependence of the reaction rate (0–5 min) of formation of DTBQ on the concentration of **1^{SQ}-PF** = 125–750 μM (red dots) and **1-PF** = 250–750 μM (blue triangles), c(DTBP-H) = 25 mM, c(NEt₃) = 50 mM.

addition of substrate (50 equiv) and base (100 equiv) under O₂ the formation of quinone is observed (Figure S39).

Of key importance with regard to the proposed reaction mechanism is also the nature of oxygen intermediates. Relevant information regarding this point can be derived from spectroscopic or kinetic data. As no copper-oxygen intermediates could be isolated at low temperature (Figure S44–S49), kinetic measurements with **1-PF** were conducted (for more details see Supporting Information). The reaction order with respect to Cu was determined with **1-PF**, which showed the highest activity of the presented systems. Moreover, to exclude the influence of the induction period and bypass the underlying preliminary reaction sequence (Scheme 4 top), the Cu^{II}-SQ complex (**1^{SQ}-PF**, Scheme 4, **a′**) was employed as catalyst, similar to the proposed intermediate **a**.

At concentrations up to approx. 600 μM a *linear* (first-order) dependence of the reaction rate on the concentration of **1^{SQ}-PF** was determined (Figure 7, red). This indicates that the conversion of the substrate to the *o*-quinone (catalytic cycle, Scheme 4 bottom) in fact occurs through a mononuclear copper(II) species. If **1-PF** is employed instead of **1^{SQ}-PF**, a linear dependence of the reaction rate is observed as well (Figure 7, blue) but, as expected, with lower values. This suggests that the preliminary reaction sequence (Scheme 4 top) also follows a mononuclear mechanism. Nevertheless, it could still be mediated by a dinuclear copper-oxygen species if formation of a primary, mononuclear CuO₂ adduct is rate-limiting.[48] Notably, the formation of (mononuclear) Cu^{II}-SQ species resulting from monooxygenation of a phenolic substrate coordinated to a dinuclear μ-η²:η²-peroxo/bis(μ-oxo) complex has been observed before in small-molecule model systems of TY.[13,14,49,50] In tyrosinase itself, a SQ intermediate formed by oxygenation of a tyrosine residue of the Caddie protein has been detected as well. This reaction appears to play an important role in the activation of this enzyme.[49]
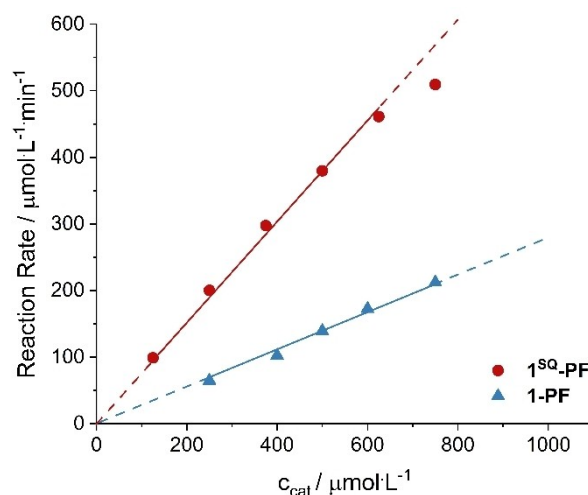
Since DTBP-H is an electron-rich substrate, it is of interest to determine whether other, especially less electron-rich substrates can be oxygenated as well. Hence, the reactivity of **1-PF** was investigated regarding the monooxygenation of a series of different phenols (3-*tert*-butylphenol (3TBP-H), 4-methoxyphenol (MeOP-H), 4-*tert*-butylphenol (4TBP-H), 4-methylphenol (MeP-H) and phenol (PhOH)). Conversion to the corresponding oxygenation products could be observed for all substrates (Figures S24–S36). As expected, a higher yield and rate were obtained with the more activated substrate MeOP-H (49%), whereas less activated substrates led to lower yields (4TBP-H: 30%, 3TBP-H: 24%, MeP-H: 18%, PhOH: 14%) and rates than obtained for DTBP-H (Table S3), which is in line with an electrophilic character of a copper(II)-O₂ intermediate involved in the catalytic cycle (Scheme 4 bottom). This is supported by a Hammett style analysis giving a negative Hammett parameter ρ (Figures S37). Moreover, an inverse kinetic isotope effect of $k_{H/D} = 0.85$ was determined by using 2D-4-*tert*-butylphenol as substrate[14,51] (for more details see Supporting Information), reflecting a rate-limiting formation of the σ-complex (Scheme 4, **d**) by attack of the electrophilic CuO₂ species.[52] Finally, low-temperature UV/Vis measurements with **1-PF** and 3TBP-H, resp., MeP-H as well as NEt₃ (4 equiv each) confirmed the SQ formation preceding that of quinone (Figure S43), as found with DTBP-H as substrate (Scheme 4 top).

Conclusion

In this study, a new protocol is presented for the synthesis of the Cu^I salts [Cu(CH₃CN)₄]**PF** (**1-PF**), [Cu(*o*DFB)₂]**PF** (**2-PF**) and the unique, linear bis-triethylamine Cu^I complex [Cu(NEt₃)₂]**PF** (**3-PF**). Investigations regarding the tyrosinase-like activity of these and Cu^I salts [Cu(CH₃CN)₄]X with

"classic" anions $X = BF_4^-$, OTf$^-$ and PF$_6^-$ showed that (i) the counterion has an influence on the product yield (*anion effect*) and the highest catalytic activity of the [Cu-(CH$_3$CN)$_4$]$^+$ complex is achieved with the aluminate counterion; (ii) for catalysts with this counterion, the initial reaction rate depends on the ligands (CH$_3$CN, *o*DFB, NEt$_3$; *ligand effect*); (iii) the formation of the quinone product (DTBQ) is linearly dependent on the (pre)catalyst concentration and therefore proceeds via a mononuclear mechanism; and (iv), if Cu^{II}-SQ complexes **1^{SQ}-PF** and **2^{SQ}-PF** are employed as catalysts for the monooxygenation of DTBP-H, similar yields, but much higher initial reaction rates are observed than for the parent Cu^I salts. This can be explained by an induction period in which the latter are converted to Cu^{II}-SQ complexes. The corresponding preliminary reaction sequence thus can be bypassed by directly using **1^{SQ}-PF** and **2^{SQ}-PF**.

Based on the experimental results, including a Hammett analysis and a kinetic isotope experiment, we propose a mechanism of the copper-mediated conversion of monophenols to *o*-quinones starting from simple copper(I) salts. Importantly, the involved catalytic cycle only contains monomeric, mono-cationic Cu^{II} complexes, which are particularly well stabilized by weakly coordinating anions, in agreement with the observed increased activities of such species when this type of anion is employed. Moreover, the proposed reaction path differs from the well-established dinuclear mechanism of phenol monooxygenation, mediated by the type3 copper protein TY. Instead, it follows the other known copper-based pathway of phenol monooxygenation in nature, which is associated with the TPQ cofactor biosynthesis in AO. Whereas the reaction mediated by that enzyme is stoichiometric, our results demonstrate that this scenario can well be turned into an efficient catalytic mode in biomimetic copper chemistry.

Conflict of Interest

The authors declare no conflict of interest.

Data Availability Statement

Research data are not shared.

[1] L. Marais, H. C. M. Vosloo, A. J. Swarts, *Coord. Chem. Rev.* **2021**, *440*, 213958.

[2] L. M. Mirica, X. Ottenwaelder, T. D. P. Stack, *Chem. Rev.* **2004**, *104*, 1013.

[3] E. I. Solomon, D. E. Heppner, E. M. Johnston, J. W. Ginsbach, J. Cirera, M. Qayyum, M. T. Kieber-Emmons, C. H. Kjaergaard, R. G. Hadt, L. Tian, *Chem. Rev.* **2014**, *114*, 3659.

[4] a) H. Decker, T. Schweikardt, F. Tuczek, *Angew. Chem. Int. Ed.* **2006**, *45*, 4546; *Angew. Chem.* **2006**, *118*, 4658; b) C. E. Elwell, N. L. Gagnon, B. D. Neisen, D. Dhar, A. D. Spaeth, G. M. Yee, W. B. Tolman, *Chem. Rev.* **2017**, *117*, 2059.

[5] M. Rolff, J. Schottenheim, H. Decker, F. Tuczek, *Chem. Soc. Rev.* **2011**, *40*, 4077.

[6] J. N. Hamann, B. Herzigkeit, R. Jurgeleit, F. Tuczek, *Coord. Chem. Rev.* **2017**, *334*, 54.

[7] L. M. Berreau, S. Mahapatra, J. A. Halfen, R. P. Houser, J. V. G. Young, W. B. Tolman, *Angew. Chem. Int. Ed.* **1999**, *38*, 207; *Angew. Chem.* **1999**, *111*, 180.

[8] a) J.-S. Taylor, *Science* **2015**, *347*, 824; b) C. J. Coates, J. Nairn, *Dev. Comp. Immunol.* **2014**, *45*, 43; c) L. Cerenius, K. Söderhäll, *Dev. Comp. Immunol.* **2021**, *122*, 104098.

[9] M. Réglier, C. Jorand, B. Waegell, *J. Chem. Soc. Chem. Commun.* **1990**, 1752.

[10] a) E. Lo Presti, M. L. Perrone, L. Santagostini, L. Casella, E. Monzani, *Inorg. Chem.* **2019**, *58*, 7335; b) M. L. Perrone, E. Salvadeo, E. Lo Presti, L. Pasotti, E. Monzani, L. Santagostini, L. Casella, *Dalton Trans.* **2017**, *46*, 4018.

[11] W. Keown, J. B. Gary, T. D. P. Stack, *J. Biol. Inorg. Chem.* **2017**, *22*, 289.

[12] L. M. Mirica, M. Vance, D. J. Rudd, B. Hedman, K. O. Hodgson, E. I. Solomon, T. D. P. Stack, *Science* **2005**, *308*, 1890.

[13] M. S. Askari, L. A. Rodríguez-Solano, A. Proppe, B. McAllister, J.-P. Lumb, X. Ottenwaelder, *Dalton Trans.* **2015**, *44*, 12094.

[14] M. S. Askari, K. V. N. Esguerra, J.-P. Lumb, X. Ottenwaelder, *Inorg. Chem.* **2015**, *54*, 8665.

[15] P. Liebhäuser, K. Keisers, A. Hoffmann, T. Schnappinger, I. Sommer, A. Thoma, C. Wilfer, R. Schoch, K. Stührenberg, M. Bauer, M. Dürr, I. Ivanović-Burmazović, S. Herres-Pawlis, *Chem. Eur. J.* **2017**, *23*, 12171.

[16] a) M. Paul, M. Teubner, B. Grimm-Lebsanft, C. Golchert, Y. Meiners, L. Senft, K. Keisers, P. Liebhäuser, T. Rösener, F. Biebl, S. Buchenau, M. Naumova, V. Murzin, R. Krug, A. Hoffmann, J. Pietruszka, I. Ivanović-Burmazović, M. Rübhausen, S. Herres-Pawlis, *Chem. Eur. J.* **2020**, *26*, 7556; b) S. Herres-Pawlis, U. Flörke, G. Henkel, *Eur. J. Inorg. Chem.* **2005**, 3815.

[17] S. Herres-Pawlis, P. Verma, R. Haase, P. Kang, C. T. Lyons, E. C. Wasinger, U. Flörke, G. Henkel, T. D. P. Stack, *J. Am. Chem. Soc.* **2009**, *131*, 1154.

[18] a) N. Fujieda, K. Umakoshi, Y. Ochi, Y. Nishikawa, S. Yanagisawa, M. Kubo, G. Kurisu, S. Itoh, *Angew. Chem. Int. Ed.* **2020**, *59*, 13385; *Angew. Chem.* **2020**, *132*, 13487; b) A. Arnold, C. Limberg, R. Metzinger, *Inorg. Chem.* **2012**, *51*, 12210.

[19] a) Y. Matoba, T. Kumagai, A. Yamamoto, H. Yoshitsu, M. Sugiyama, *J. Biol. Chem.* **2006**, *281*, 8981; b) E. A. Lewis, W. B. Tolman, *Chem. Rev.* **2004**, *104*, 1047.

[20] B. Herzigkeit, R. Jurgeleit, B. M. Flöser, N. E. Meißner, T. A. Engesser, C. Näther, F. Tuczek, *Eur. J. Inorg. Chem.* **2019**, 2258.

[21] a) J. N. Hamann, M. Rolff, F. Tuczek, *Dalton Trans.* **2015**, *44*, 3251; b) J. N. Hamann, R. Schneider, F. Tuczek, *J. Coord. Chem.* **2015**, *68*, 3259; c) J. N. Hamann, F. Tuczek, *Chem. Commun.* **2014**, *50*, 2298; d) J. Schottenheim, C. Gernert, B. Herzigkeit, J. Krahmer, F. Tuczek, *Eur. J. Inorg. Chem.* **2015**, 3501.

[22] F. Wendt, C. Näther, F. Tuczek, *J. Biol. Inorg. Chem.* **2016**, *21*, 777.

[23] B. Herzigkeit, B. M. Flöser, T. A. Engesser, C. Näther, F. Tuczek, *Eur. J. Inorg. Chem.* **2018**, 3058.

[24] B. Herzigkeit, B. M. Flöser, N. E. Meißner, T. A. Engesser, F. Tuczek, *ChemCatChem* **2018**, *10*, 5402.

[25] J. E. Bulkowski, US-Patent 4.545.937, **1985**.

[26] a) T. A. Engesser, C. Friedmann, A. Martens, D. Kratzert, P. J. Malinowski, I. Krossing, *Chem. Eur. J.* **2016**, *22*, 15085; b) T. Köchner, T. A. Engesser, H. Scherer, D. A. Plattner, A. Steffani, I. Krossing, *Angew. Chem. Int. Ed.* **2012**, *51*, 6529; *Angew. Chem.* **2012**, *124*, 6635.

[27] I. M. Riddlestone, A. Kraft, J. Schaefer, I. Krossing, *Angew. Chem. Int. Ed.* **2018**, *57*, 13982; *Angew. Chem.* **2018**, *130*, 14178.

[28] a) S. P. Smidt, N. Zimmermann, M. Studer, A. Pfaltz, *Chem. Eur. J.* **2004**, *10*, 4685; b) M. Huber, A. Kurek, I. Krossing, R. Mülhaupt, H. Schnöckel, *Z. Anorg. Allg. Chem.* **2009**, *635*, 1787; c) D. S. McGuinness, A. J. Rucklidge, R. P. Tooze, A. M. Z. Slawin, *Organometallics* **2007**, *26*, 2561; d) Y. Li, M. Cokoja, F. E. Kühn, *Coord. Chem. Rev.* **2011**, *255*, 1541; e) I. Krossing, L. van Wüllen, *Chem. Eur. J.* **2002**, *8*, 700.

[29] Y. Li, B. Diebl, A. Raith, F. E. Kühn, *Tetrahedron Lett.* **2008**, *49*, 5954.

[30] J. P. Klinman, F. Bonnot, *Chem. Rev.* **2014**, *114*, 4343.

[31] J. L. DuBois, J. P. Klinman, *Arch. Biochem. Biophys.* **2005**, *433*, 255.

[32] B. J. Brazeau, B. J. Johnson, C. M. Wilmot, *Arch. Biochem. Biophys.* **2004**, *428*, 22.

[33] K. Tabuchi, M. Z. Ertem, H. Sugimoto, A. Kunishita, T. Tano, N. Fujieda, C. J. Cramer, S. Itoh, *Inorg. Chem.* **2011**, *50*, 1633.

[34] D. M. Dooley, *J. Biol. Inorg. Chem.* **1999**, *4*, 1.

[35] J. L. DuBois, J. P. Klinman, *Biochemistry* **2005**, *44*, 11381.

[36] a) W. Beck, K. Suenkel, *Chem. Rev.* **1988**, *88*, 1405; b) S. Alvarez, *Chem. Eur. J.* **2020**, *26*, 4350; Erratum: S. Alvarez, *Chem. Eur. J.* **2020**, *26*, 8663.

[37] G. Santiso-Quiñones, A. Higelin, J. Schaefer, R. Brückner, C. Knapp, I. Krossing, *Chem. Eur. J.* **2009**, *15*, 6663.

[38] I. Krossing, *J. Am. Chem. Soc.* **2001**, *123*, 4603.

[39] M. Elsayed Moussa, M. Piesch, M. Fleischmann, A. Schreiner, M. Seidl, M. Scheer, *Dalton Trans.* **2018**, *47*, 16031.

[40] a) B. J. Hathaway, D. G. Holah, A. E. Underhill, *J. Chem. Soc.* **1962**, 2444; b) A. M. Wright, G. Wu, T. W. Hayton, *J. Am. Chem. Soc.* **2010**, *132*, 14336.

[41] a) A. Kunze, R. Gleiter, F. Rominger, *Chem. Commun.* **1999**, 171; b) A. Kunze, S. Balalaie, R. Gleiter, F. Rominger, *Eur. J. Org. Chem.* **2006**, 2942.

[42] a) B. Gomez-Lor, M. Iglesias, C. Cascales, E. Gutierrez-Puebla, M. A. Monge, *Chem. Mater.* **2001**, *13*, 1364; b) G. Margraf, J. W. Bats, M. Bolte, H.-W. Lerner, M. Wagner, *Chem. Commun.* **2003**, 956; c) S.-L. Zheng, M. Messerschmidt, P. Coppens, *Angew. Chem. Int. Ed.* **2005**, *44*, 4614; *Angew. Chem.* **2005**, *117*, 4690.

[43] Deposition Number 2103688 contains the supplementary crystallographic data for this paper. These data are provided free of charge by the joint Cambridge Crystallographic Data Centre and Fachinformationszentrum Karlsruhe Access Structures service.

[44] T. A. Engesser, M. R. Lichtenthaler, M. Schleep, I. Krossing, *Chem. Soc. Rev.* **2016**, *45*, 789.

[45] T. G. Gaule, M. A. Smith, K. M. Tych, P. Pirrat, C. H. Trinh, A. R. Pearson, P. F. Knowles, M. J. McPherson, *Biochemistry* **2018**, *57*, 5301.

[46] M. Kim, T. Okajima, S. Kishishita, M. Yoshimura, A. Kawamori, K. Tanizawa, H. Yamaguchi, *Nat. Struct. Mol. Biol.* **2002**, *9*, 591.

[47] S. V. Jovanovic, K. Kónya, J. C. Scaiano, *Can. J. Chem.* **1995**, *73*, 1803.

[48] a) K. D. Karlin, N. Wei, B. Jung, S. Kaderli, A. D. Zuberbuehler, *J. Am. Chem. Soc.* **1991**, *113*, 5868; b) M. Rolff, J. Schottenheim, G. Peters, F. Tuczek, *Angew. Chem. Int. Ed.* **2010**, *49*, 6438; *Angew. Chem.* **2010**, *122*, 6583.

[49] Y. Matoba, S. Kihara, Y. Muraki, N. Bando, H. Yoshitsu, T. Kuroda, M. Sakaguchi, K. Kayama, H. Tai, S. Hirota, T. Ogura, M. Sugiyama, *Biochemistry* **2017**, *56*, 5593.

[50] P. Verma, J. Weir, L. Mirica, T. D. P. Stack, *Inorg. Chem.* **2011**, *50*, 9816.

[51] A. Hoffmann, C. Citek, S. Binder, A. Goos, M. Rübhausen, O. Troeppner, I. Ivanović-Burmazović, E. C. Wasinger, T. D. P. Stack, S. Herres-Pawlis, *Angew. Chem. Int. Ed.* **2013**, *52*, 5398; *Angew. Chem.* **2013**, *125*, 5508.

[52] E. V. Anslyn, D. A. Dougherty, *Modern physical organic chemistry*, University Science Books, Mill Valley, **2006**.